Domain-growth kinetics and aspects of pinning: A Monte Carlo simulation study

Teresa Castán
Departament d'Estructura i Constituents de la Matèria, Facultat de Física, Universitat de Barcelona, Diagonal 647, E-08028 Barcelona, Catalonia, Spain

Per-Anker Lindgård
Physics Department, Risø National Laboratory, Roskilde, DK-4000, Denmark
(Received 12 April 1990; revised manuscript received 23 July 1990)

By means of Monte Carlo computer simulations we study the domain-growth kinetics after a quench across a first-order line to very low and moderate temperatures in a multidegenerate system with nonconserved order parameter. The model is a continuous spin model relevant for martensitic transformations, surface reconstructions, and magnetic transitions. No external impurities are introduced, but the model has a number of intrinsic, annealable pinning mechanisms, which strongly influences the growth kinetics. It allows a study of pinning effects of three kinds: (a) pinning of domain walls by defects—this is found in effect to stop the growth, forming a metastable state at low temperatures T; (b) temporary pinning by stacking faults or zero-curvature domain walls; and (c) topological pinnings, which are also found to be temporary. These just slow down the growth. The pinning mechanisms and the depinning probability at higher temperatures are studied. The excess energy of the domain walls is found to follow an algebraic decay $\Delta E(t)=E_M+At^{-n}$, with $E_M=0$ for cases (b) and (c) and decaying toward a metastable state with energy $E_M\neq 0$ for case (a). The exponent is found to cross over from $n=\frac{1}{4}$ at $T\sim 0$ to $n=\frac{1}{2}$ with temperature for models with pinnings of types (a) and (b). For topological pinnings at $T\sim 0$, n is consistent with $n=\frac{1}{8}$, a value conceivable for several levels of hierarchically interrelated domain-wall movement. When the continuous-spin model is reduced to a discrete Potts-like model, with the same parameters, the exponent is found to be consistent with the classical Allen-Cahn exponent $n=\frac{1}{2}$.

I. INTRODUCTION

Kinetics of domain growth has in recent years been intensively studied by Monte Carlo simulation techniques[1–9] in the search for universality classes. The time dependence of the excess domain-wall energy $\Delta E(t)$ has been studied and shown to be consistent with an algebraic decay law $\Delta E(t)=At^{-n}$. For curvature-driven growth (and nonconserved order parameter), systems[10] have been found to follow the Allen-Cahn[11] behavior with $n=\frac{1}{2}$, but also systems have been found with a slower growth. An interesting slow-growth class with $n=\frac{1}{4}$ was discovered by Mouritsen.[12] It was analyzed[13] and found to be represented by a singular Allen-Cahn case, in which straight domain walls, corresponding to stacking faults or twin boundaries, give rise to temporary pinning effects, in the sense that the movement of the domain walls is hierarchical. For quenches to very low temperatures, this pinning slows down the growth, but does not hamper it totally. At higher tempertures,[14] the Allen-Cahn growth with $n=\frac{1}{2}$ is recovered. However, systems with even slower growth than $n=\frac{1}{4}$ have been found.[15] For a multidegenerate system, it has been suggested that the vortices, where three or more different phases meet, act as pinning centers, slowing down the growth dynamics. In the framework of the Q-state Potts model, Safran[16] predicted that when $Q>d+1$, d being the dimensionality of the system, the growth at late times is logarithmic. Although this effect has not been observed in simulations of the Potts model,[17] it might be operative in other situations. We would like, here, to study the role that the vortices have on the kinetics of domain growth in a different model. Pinnings exist, but are not found to be definitive.

Although by now very much is known about the ordering kinetics of simple models, such as the Ising model,[2,9,18–20] the Potts model,[7,8,17] and the axial next-nearest-neighbor Ising ANNNI model,[5,6] and the effect of quenched (immobile) impurities[4,21] and random fields,[22] the effects of annealed (mobile) defects on the time evolution has received relatively little attention.[2,3,23] However, it is important to understand this is in order to correctly interpet the experimental results on domain growth. For quenches to very low temperatures, it is generally accepted that both quenched and annealed defects will pin the domain walls and give rise to the slowest possible growth of the domains, namely a logarithmic growth. However, for most practical purposes, and not astronomical time scales, the systems can be assumed to end in a metastable, final state with, in effect, no further growth. We shall adopt this picture in this paper.

In our model, pinning centers on the domain walls can be studied. They are intrinsic properties of the model; they correspond to defect pinnings in an experimental situation and simulate, as well, important aspects of annealed external impurities. The defects are, in principle, mobile (depending on the temperature), and the model is

describing a situation quite different from that studied in the random-field problem[22] with static, fixed defects or impurities. At $T \simeq 0$, some of the pinning centers in the model become immobile. One of the purposes of this paper is to investigate, for a twofold degenerate system, the effect of drastic pinnings, which stop the growth (i.e., give only logarithmic growth) and leave the system in an essentially infinitely long-lived metastable state consisting of a "polycrystal" with pinned domain walls or grain boundaries. We will show that at very low temperatures the defect pinning centers, in interplay with the temporary pinnings constituted by the stacking faults (straight walls), in effect, stop the growth in a metastable state. It is important that the energy E_M of this can be fairly accurately estimated. The growth toward this state corresponds to a minimalization of the domain-wall length between the pinning centers. It proceeds following the normal, i.e., unpinned behavior. The growth law is therefore of the type $\Delta E(t) = At^{-n} + E_M$. Since it is, in experiment or simulation, very difficult to distinguish this growth law from $\Delta E(t) = A't^{-n'}$ with an effective exponent $n' < n$, it is crucial to have a knowledge of the energy E_M of the final state in order to determine the correct growth exponent. This problem is particularly important for analyzing an experimental situation, where there will always be a number of defects and impurities present that give rise to pinning effects. However, it is still possible, in principle, and with great care, to extract the ideal algebraic growth behavior from the approach toward the logarithmic regime with effectively no growth.

Experimentally, $\Delta E(t)$ is not easily obtainable. But, if we assume that the growth follows the scaling behavior necessary for the algebraic time evolution, other quantities, e.g., the domain radius or the structure factor, will exhibit the same exponent. Our conclusions obtained by studying the self-averaging[24] $\Delta E(t)$ are therefore expected to hold more generally. Experiments on ordering kinetics in impure chemisorbed overlayers[25] and off-stochiometric alloys[26] suggest that annealed, mobile impurities lead to a slow growth tending toward an effective logarithmic growth law, in agreement with recent Monte Carlo simulations[2] in a dilute Ising model. Measurements on grain-boundary migration in Pb (Ref. 27) and Sn (Ref. 28) show slow kinetics, as do experimental studies of grain growth kinetics in polycrystalline materials[29] concerning systems that have a high ground-state degeneracy. It might be fruitful to reanalyze the experiments in the light of the present investigation.

II. THE MODEL

We wish to study a magnetic model Hamiltonian, which, besides describing magnetic transitions,[30] is also useful for describing displacive structural transitions[15,31] and domain growth.[13,14] Therefore we use a language relevant to both cases. In the model there is a competition between an interaction K, favoring ferromagnetic (FM) (called square in Ref. 13.) structure in the z direction, a pseudo dipolar interacton J, favoring an antiferromagnetic (AFM) (called triangular in Ref. 13.) structure in the x-y plane, and finally an anisotropy term D ($=2J$), which is introduced in order to reduce the number of equivalent AFM domains to four. The interactions are between nearest neighbors. The AFM structure consists of ferromagnetically aligned spin chains stacked with alternating directions. The Hamiltonian is

$$H = \sum_{i,j} J[\mathbf{S}_i \cdot \mathbf{S}_j - P(\mathbf{S}_i \cdot \mathbf{r}_{ij})(\mathbf{S}_j \cdot \mathbf{r}_{ij})] - \sum_{i,j} K S_i^z S_j^z - D \sum_i [(S_i^x)^4 + (S_i^y)^4] \ . \quad (1)$$

This Hamiltonian, apart from being physically relevant, has a rich spectrum of possibilities for studying pinning effects on domain growth. For the dipole parameter $P=3$, the AFM domain walls are of two kinds: broad soliton walls with spins turning out of the x-y plane into the $+z$ or $-z$ directions for mismatch on an aligned chain along the x or y direction, and sharp walls for a twin boundary or a stacking fault in the sequence of the chains. The model can be simplified further by reducing the spin degrees of freedom in order to study selected effects.

I. First, consider only continuous spins in the upper half of the x-z plane. We call this model I or ($\pm x,z$, and continuous). This can separately demonstrate the interplay between the broad curved walls and the sharp straight walls, where the first have to wait for the straight walls to disappear before being able to reduce their length. We call this temporary pinning effect, and it was shown[13] that this hierarchical behavior alters, for all times, the time evolution exponent to $n = \frac{1}{4}$ for quenches to very low temperatures. At high temperatures, the standard Allen-Cahn exponent $n = \frac{1}{2}$ is recovered.

II. In model II ($\pm x$, $\pm z$, and continuous), we allow the soliton walls to deviate both in the $+z$ and $-z$ direction, and we allow continuous-spin directions in the full x-z plane. This gives rise to an interesting pinning center on the walls, when two oppositely oriented soliton walls meet. Although it is an intrinsic property of the model, it is closely related to defect and impurity pinnings. When combined with the temporary pinning of the stacking faults in model I, it leads to an effective stop of the growth, i.e., a logarithmic growth.

III. The full model III ($\pm x$, $\pm y$, $\pm z$, continuous, and $P=3$) with continuous spins in the full space, combines these effects and has, in addition, a possible topological pinning, namely, where the four types of AFM domains ($+x$, $-x$, $+y$, and $-y$) meet in a vortex point.

IV. In order to study the topological pinning separately, we can consider a full model IV, with $P=2$ ($\pm x$, $\pm y$, $\pm z$, continuous, and $P=2$). For this value of P, all walls are essentially equal and sharp. The spins in the AFM domains prefer to meet at an angle of 90°, and therefore topological pinning centers of the vortex type are formed where four domains meet. We will also study a further restricted model, called the Potts model IV ($\pm x$, $\pm y$, $\pm z$, discrete, and $P=2$), in which we only allow the spins to assume the discrete $\pm x$, $\pm y$, and $\pm z$ directions.

In Fig. 1, we show the phase diagram for the three models with $P=3$. The phase diagram for the full model

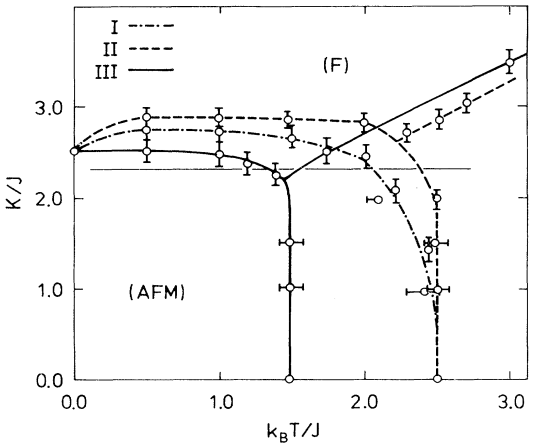

FIG. 1. The phase diagrams for the models I, II, and III described in the text. The quenches are performed along the line at $K/J=2.3$.

III ($P=3$) is apart from a simple scaling identical to the full model IV ($P=2$) which was studied previously.[31] We perform temperature quenches along the path indicated at $K/J=2.3$. For model IV, $K/J=1.8$ was chosen.[31] The path crosses a first-order transition line between the FM phase, corresponding to the cubic, and the AFM phase, corresponding to the hexagonal phases, in an analogous way as in the martensitic transformation. The relevance of the magnetic model for this transition problem has been investigated elsewhere.[15,31] Here we will focus our attention on the self-pinning aspects of the models and the influence on the domain growth that follows after a rapid quench from the disordered phase to different temperatures in the AFM phase. An interesting special feature of the restricted models I and II is the reentrance of the FM phase at low temperatures. Such a behavior has not been observed in experimental magnetic or martensitic transformations, but it is conceivable. It is caused by entropy stabilization of the AFM phase, when the order-parameter variables are restricted to a plane, giving a model similar to an XY model.

III. MONTE CARLO SIMULATION RESULTS

Using standard Monte Carlo (MC) simulation techniques,[32,33] we follow the time evolution of the domain growth after quenches from a high temperature in the disordered phase to different low temperatures in the AFM phase. Our system is a set of N spins on a square two-dimensional lattice, subject to periodic boundary conditions. The unit of time, one Monte Carlo step per spin (MCS), is defined as N attempts to flip N spins sequentially. First, in Sec. III A we discuss quenches to very low temperatures ($T\simeq 0$), where the pinning is, in effect, definitive. Second, in Sec. III B we discuss the results corresponding to quenches to finite temperature, where the pinning ceases to be effective. In Secs. III C and III D, we discuss the various pinning mechanisms.

A. Quenches to very low temperatures ($T\simeq 0$)

In this section we present the statistical analyses of the MC simulation from the disordered phase to well inside the AFM phase at $T=0.02J/k_B=0.008T_C$ along the path indicated in Fig. 1: k_BT_C is $2.4J$. If a quench has been performed at $t=0$, the excess energy at time t is defined as

$$\Delta E(t)=E(t)-E_T(\infty)\ , \tag{2}$$

where $E_T(\infty)$ is the equilibrium energy at the quench temperature T. The decay is furthermore usually expected to follow a power-law:

$$\Delta E(t)=A't^{n'}\ . \tag{3}$$

This definition presupposes that the system evolves to reach the one-domain equilibrium state for the temperature T, at $t=\infty$. The $E_T(\infty)$ for this state is easily calculated by the Monte Carlo simulation. Figure 2 shows a log-log plot of the time evolution of $\Delta E(t)$ for models II and III. Results corresponding to model I were reported in Ref. 13. For model II we have used both $N=100\times 100$ and 200×200 size systems; for model III only, $N=100\times 100$. The result of a least-squares fit for obtaining the exponent n for Eq. (3) is shown above each curve. For model II we have averaged over 15 different runs for the 100×100 system and over five runs for the 200×200 system. For model III the fit has been obtained from an average over eight runs of the 100×100 systems. A common feature is the clear crossover at a time $t=t^*$, from an early time regime with exponent n_1 to a slower decay with exponent n_2. It has been demonstrated[13] that

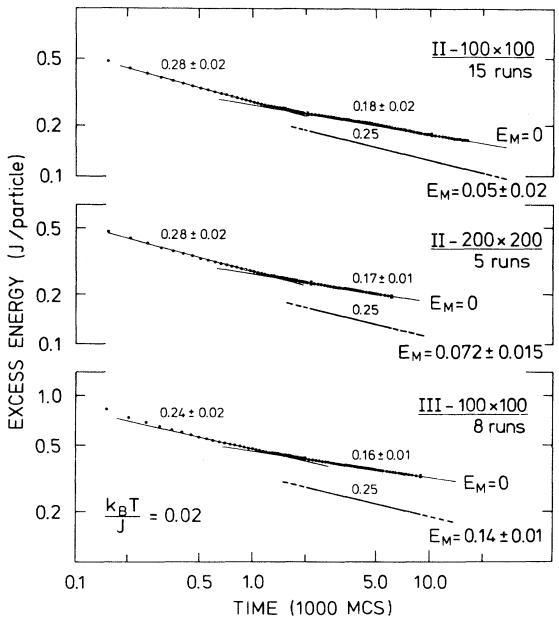

FIG. 2. The excess energy $\Delta E(t)$ for the models II and III for quenches to $T=0.008T_C$. Error bars are indicated at 2000 and 10 000 MCS for $N=100\times 100$ and at 2000 and 7000 MCS for $N=200\times 200$.

n_1 is an effective "exponent" which, in fact, represents an exponentially fast optimization of the width of the domain walls and of the order inside the domains. It is not relevant for the time evolution of the domain-wall system as such. We obtain $t^*=1200\pm300$ MCS for $N=100\times100$ for both models II and III, and, consistently, $t^*=1100\pm200$ MCS for the model-II 200×200 system. The crossover does not significantly depend on the size of the system. The least-squares fit to Eq. (3) gives the late-time exponents for model II, $n_2=0.18\pm0.02$ for $N=100\times100$ (and, consistently, $n_2=0.17\pm0.01$ for $N=200\times200$) and for model III, $n_2=0.16\pm0.01$. These exponents are systematically smaller than the $n\sim\frac{1}{4}$ obtained[13] for model I. This n characterizes the behavior of a mixture of sharp straight walls (called S boundaries) and broad curved walls (called C boundaries) with no pinnings, see Fig. 3. Equation (3) is valid when the system evolves into the final thermodynamical equilibrium state with only one domain. However, from our simulations, we have observed that for models II and III the system rather approaches a long-lived metastable state formed by a pinned domain-wall structure. The difference between models I and II is the pinning centers residing along the broad walls preventing the broad walls to move. These were the only walls that could move. This leads to, in effect, pinned domain structure for model II, and the growth behavior crosses over from an algebraic law, of the form $\Delta E(t)=A't^{-n_2}$, to a late-time logarithmic regime. It is important that the energy of the metastable state can be accurately estimated. The final state is found from the latest-time configuration by applying the knowledge about how the walls are able to move and where they are pinned. By counting the final length L_C of the C boundary, with the energy per unit length[13] $\simeq4J$, and the final length L_S of the S boundary with energy per unit length[13] $\simeq2J$, we obtain the energy of the, in effect, final metastable state $E_M=0.08\pm0.01J$ for the 100×100, and, consistently, $E_M=0.06\pm0.02J$ for the 200×200 size system. Under the assumption that the pinning centers do not move, but rather change the final state to an effectively, stable (metastable) state corresponding to an optimal domain-wall network, the time evolution is therefore of the form

$$\Delta E(t)=At^{-n}+E_M \ . \tag{4}$$

A fit to Eq. (4) with a fixed exponent $n=\frac{1}{4}$ gives the continuous line shown in Fig. 2, with a fitted residual energy $E_M=0.05\pm0.02J$ for $N=100\times100$, and, consistently, $E_M=0.07\pm0.02J$ for the $N=200\times200$ system. These values of E_M agree within the statistical errors with the E_M directly evaluated from our simulations. The time evolution towards the, in effect, final state, therefore is consistent with the unpinned time evolution of model I with $n=\frac{1}{4}$. After this state has been reached, further evolution proceeds logarithmically slow with no effective growth. As a test we have also tried a fit to Eq. (4) with the conventional Allen-Cahn exponent $n=\frac{1}{2}$. This corresponds to the analysis proposed by Kaski *et al.*[19] Here, we have identified the arbitrary constant used there[19] as the residual energy of the metastable state. In the fit with fixed $n=\frac{1}{2}$, we obtain $E_M=0.13\pm0.02J$, which is much larger than the residual energy estimated from the configurations in the simulations. To show the relative quality of the different fits, the deviations are plotted in Fig. 4, as a check for systematic deviations. The data alone do not allow a distinction between the first two fits

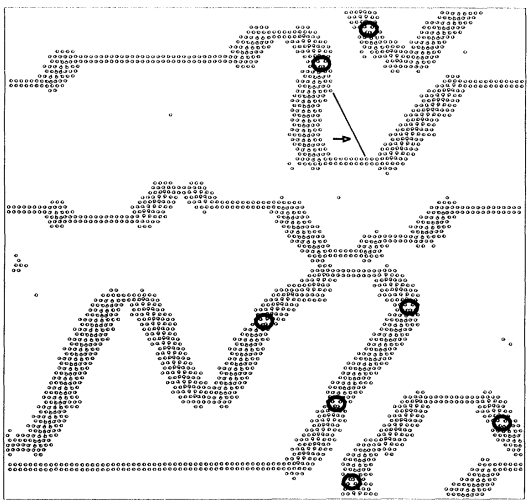

FIG. 3. A typical late-time MC result for model II showing pinning centers on the broad soliton walls, indicated by large open circles surrounding two oppositely aligned spins. The spins are shown as-○; only the disordered spins are shown, i.e., the walls. The details in their definition are given in Ref. 13. The spins deviate in the x-z plane, but are, for illustrative purposes, shown in the displayed x-y plane; see Fig. 6 for a magnified plot. The pinning centers do not move at low temperature. Some small movements of the broad walls are still possible. The arrow indicates one of these. However, the *de facto* final metastable state can be predicted and the energy estimated.

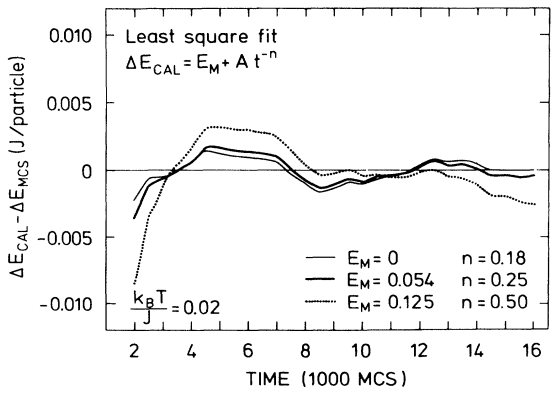

FIG. 4. The deviations for three different least-squares fit to the late-time data for model II (Fig. 2). The thick line is for fixed $n=\frac{1}{4}$, thin line for fixed residual energy $E_M=0$, and the dotted line for a fit with fixed $n=\frac{1}{2}$.

(thin and thick lines). The estimate of the residual energy E_M favors the fit with $n=\frac{1}{4}$. However, the fit with fixed $n=\frac{1}{2}$ is clearly worse (dotted line), where both the systematic deviations and the E_M are too large. Consequently, the exponent $n=\frac{1}{2}$ is not consistent with the simulation results of model II, which is to be expected on the basis of the results of model I giving $n=\frac{1}{4}$. This analysis shows that it is difficult, but possible, to extract the growth law from the behavior of the approach toward, in effect, a pinned metastable state. It is somewhat related to the previously discussed[13,20] analysis of the "slab" effect due to the periodic boundary conditions. However, in the pinning case, it is a real physical effect.

The complexity of the wall structure exhibited by model III makes it more difficult to predict the final pinned state and therefore to estimate the length of the remaining domain walls. A least-squares fit with fixed $n=\frac{1}{4}$ gives $E_M=0.14\pm0.01J$. The remaining energy is clearly larger than for model II, as expected. In model III there might also be an effect of a topological pinning, which could effect the value of n. We return to this question in an analysis of the simpler model IV.

B. Quenches to finite temperatures

In order to study the behavior of the system, and in particular of the pinning centers, as a function of the quench temperature T we have followed the time evolution of model II, with $N=100\times100$ up to $T=0.2T_C$. In Fig. 5 we show the temperature dependence of the growth exponent. The solid circles represent the exponent obtained from a least-squares fit with $E_M=0$ averaged over 15 runs. The exponent increases with temperature and exhibits around $T=0.08T_C$ an additional abrupt crossover, which is indicative of the onset of an activated hopping of the pinning centers. The continuous thin line[14] corresponds to the smooth crossover found for model I. The dot-dashed line is the assumed "nonpinned" behavior of model II if no pinnings were present. By following the time evolution of the individual configurations, we observe that for $T<0.08T_C$ the pinning centers do not move, and the system is trapped in a metastable state. For higher temperatures, the centers become unpinned and do move with the C boundary. This, of course, speeds up the evolution and increases n. The behavior of the "nonpinned" curve at low temperatures, open circles in Fig. 5, has been obtained by fitting the data for $T<0.08T_C$ to Eq. (4) with $E_M=0.05J$, instead of to Eq. (3), where $E_M=0$. The exponent both for models I and II crosses over from $n=\frac{1}{4}$ at low temperatures to $n=\frac{1}{2}$ at higher temperatures. The limiting values are characteristic for curvature-driven growth. The intermediate exponents are effective. As it was shown from the analysis[13] of model I that $n=\frac{1}{4}$ characterizes a special case with a mixture of straight, temporarily pinned walls and moving curved walls. When the temperature increases,[14] the temporary pinning time of the S boundary is reduced. Additionally, the S boundary starts to "curve" by means of kinks. The hierarchical movement of the walls then becomes irrelevant, and the system approaches the standard Allen-Cahn law with $n=\frac{1}{2}$. The initial slower increase of n with temperature for model II is due to the additional pinning centers on the walls. We have analyzed the possibilities for these to move in the Appendix and find that the first jump possibility has an activation energy of about $\Delta E_{\text{barrier}}=0.02J=0.08k_BT_C$. This is in qualitative agreement with the rapid increase in n around $T=0.08T_C$.

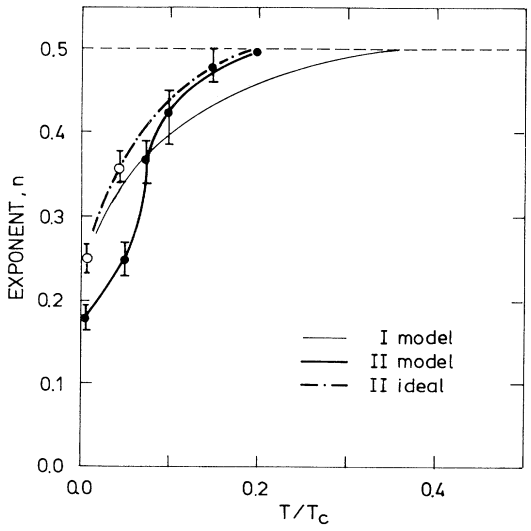

FIG. 5. The temperature variation of the exponents from $n=\frac{1}{4}$ to the Allen-Cahn exponent $n=\frac{1}{2}$ at large temperatures. The closed circles are obtained by a least-squares fit for model II, assuming $E_M=0$, and the open circles for $E_M=0.05J$. The dot-dashed line represents the behavior of model II when the pinnings are eliminated.

C. The pinning center on the soliton wall

At late times the domain-wall network consists of an interconnected mixture of S and C boundaries. This is shown in Fig. 6, which further demonstrates that a pinning center arises at the meeting point of a $+z$ and $-z$ soliton wall, indicated as soliton walls with upward- and downward-pointing deviations. The pinning center consists of the two abruptly broken chains in the middle; only the limiting spins in the domains are displayed. The configuration has a relatively small energy as discussed in the Appendix. This causes the pinning. In model I the C boundary moves with a constant velocity, which is proportional to its curvature, i.e., to $1/L_C$. Only after the S-boundary length L_S has been eliminated, the C-boundary length L_C can start to be reduced. With the additional pinning center the situation changes drastically. A typical, in effect, final metastable state can be predicted from the late-time state as shown in Fig. 3. The density of pinning points does not depend on the size of the system. We find the average number of pinning points $N^P=9\pm1$ for $N=100\times100$. They are distributed along the C boundaries with an average distance $L_C^P=42\pm6$ solitons. Consistently, for the $N=200\times200$

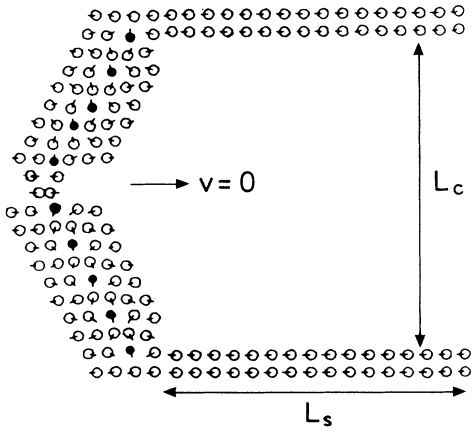

FIG. 6. Typical example from the MC simulation showing a pinning center where two oppositely pointing soliton walls meet. The deviations $+z$ and $-z$ are indicated as upward- and downward-pointing spins, here indicated as displaced atoms. The figure defines the length of the C boundary, L_C, and of the S boundary, L_S.

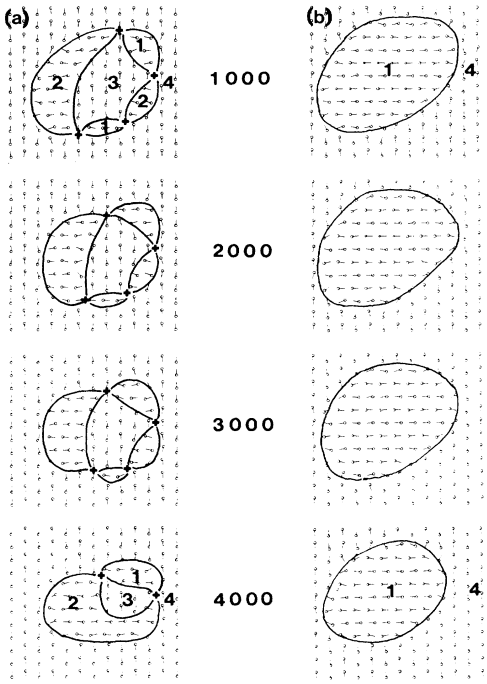

FIG. 7. The time evolution at $T=0.008T_C$ of two small domains in model IV from 1000 to 4000 MCS. (a) A domain of type 3 in a matrix of type 4 is surrounded by small domains of types 1 and 2. All four phases meet in several vortex points, which are pinned until the connecting wall angles get sufficiently small, then a small jump is made probable. (b) A domain 1 in a matrix of type 4 has sharp walls. The time evolution for (a) and (b) is similar. A similar size domain for model I will disappear in less than 1500 MCS and, in the Potts model IV, in less than 200 MCS. This shows that the configurations (a) and (b) are both pinned.

systems, we find that $N^P=28\pm3$, and $L_C^P=45\pm5$ solitons. We conclude that the drastic pinning effect is not due to a finite-size effect of the kind leading to the "slab" effect.

D. Topological pinning effects

In model IV an extremely slow growth, with $n=0.13\pm0.03$, was observed.[15] It is of interest to attempt to find the reason for this unexpected behavior. At late times, after a quench to low temperatures, the system is in a polydomain state formed by the four possible AFM domains. Let us call them 1, 2, 3, and 4 for the type $+x$, $-x$, $+y$, and $-y$ domains. The domain walls are sharp between all types of domains and are, in general, not straight. Neighboring domain numbers are not favorable. An additional domain is therefore always introduced between two in a sequence, e.g., between 3 and 4 will appear a 1 or a 2. At an intersection point all phases meet in a vortex-like structure. In Fig. 7(a), we follow the time evolution of a small, almost spherical domain found in the MC simulation. It is of type 3 in a matrix of type 4; the "domain wall" is consisting of small domains of types 1 and 2 meeting in topological pinning points. The time evolution is extremely slow compared to that for similar size domains for model I, which would disappear after less than 1500 MCS. It is observed that the walls move to reduce their curvature between the fixed pinning points. However, when the angles at the vortex becomes sufficiently small, the pinning point can make a very small jump. Then it does not move until the resulting wall curvature is still further reduced. This is in contradiction to the behavior assumed by Safran[16] in which the angles a the vortex were supposed to be constant, preventing the pinning point from moving. In this model, as in the Potts model, there is no definitive topological pinning—although a temporary one. In the Clock model, there is observed a definitive topological pinning for quenching to zero temperature,[34] but not for finite-temperature quenches.[35] It is interesting that the time evolution of a similar domain of type 1 in a matrix of 4, where there are no topological pinning centers, develops equally slow, [Fig. 7(b)]. An analysis shows that the walls are temporarily pinned at almost all points. To demonstrate this, we restrict the spins to try only the relevant $\pm x$, $\pm y$, and $\pm z$ directions, instead of allowing them to try all directions in space. This gives a model that closely resembles a Potts model. The time evolution of the small domain is now extremely fast in comparison. It is interesting that, with this restriction in the spin degrees of freedom, the model IV behaves as a standard Potts model, and that the growth exponent is (for an average of over five runs, $n=0.52\pm0.02$) quite consistent with the classical Allen-Cahn exponent and also with previous studies of the Potts model.[7,8,17] This is shown on Fig. 8. The difference between the continuous-spin model and the Potts model now becomes clear. In the Potts model, the spins are forced to attempt only the relevant flips, whereas, in the continuous model, the probability for finding the relevant flips is infinitesimally small. Only

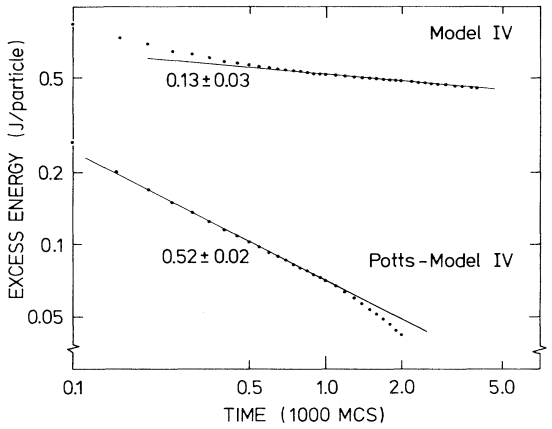

FIG. 8. A log-log plot of the excess energy for model IV and the Potts-model IV. The last has an exponent consistent with the Allen-Cahn $n=\frac{1}{2}$, whereas model IV has an exponent consistent with $n=\frac{1}{8}$. Finite-size effects are apparent for the Potts model IV for late times.

when the neighboring spin deviations are in a favorable direction does the probability of finding a relevant flip become significantly large. The wall movement therefore becomes hierarchical, depending on the curvature and the states of the neighboring several spins. We believe this causes the slow, most probably algebraic, growth. The growth is very difficult to distinguish from a logarithmic growth law of the kind $\Delta E(t)=A/\ln(Bt)$, if both constants A and B are free to be fitted. Such a behavior was suggested for zero-temperature quenches in the continuous models.[36] In Fig. 8 the time evolutions of model IV and Potts model IV are compared.

IV. DISCUSSION AND CONCLUSION

By varying the parameters and the spin degrees of freedom of the dipolar coupling model introduced[15] to describe displacive structural phase transition across a first-order line, we have been able to realize a number of effects of relevance for the domain growth after a quench to a low-temperature multidegenerate state. We have studied temporary pinning effects constituted by zero-curvature walls, pinnings of the defect kind, as well as topological pinnings. The defect pinnings are definitive, whereas the topological pinnings in our model only slow down the growth. Particularly interesting is that it is possible to derive the exponent for an ideal algebraic growth even for cases where the system is going to be pinned into, in effect, a final metastable state. In order to do this, one needs to be able to fairly accurately estimate the final-state residual energy. In case other properties are measured, a similar knowledge about the final state, residual domain radius, or structure factor, etc., is needed. We have found that, in our model, topological defects do not give rise to definitive pinning centers but only slow down the growth rate, changing the growth exponent n. A new slow-growth class probably exists between the $n=\frac{1}{4}$ class and the logarithmic growth. For model IV an exponent of $n=0.13\pm0.03$ was found.[15] The growth is here analyzed and found to be of the type of a temporary pinning, which can be removed if a hierarchy of wall movements takes place. In the simplest case where there are only two interdependent evolutions, we previously found[13] that the growth exponent reduced to $n=\frac{1}{4}$. It was suggested[13] that several levels of the hierarchy could lead to smaller exponents, such as $n=\frac{1}{8}$, etc. Model IV is consistent with $n=\frac{1}{8}$. However, it is difficult to formulate a scaling theory to substantiate this, as it was done in the case with $n=\frac{1}{4}$ for model I. The slow growth in model IV is related to the continuous-spin variables. This was demonstrated by restricting the spin variables to only the most probable directions, namely along $\pm x$, $\pm y$, and $\pm z$. Then, the model reduces effectively to a Potts model, and one retains the growth exponent $n=\frac{1}{2}$, even for low-temperature quenches. In this case, there is no hierarchical wall movement.

ACKNOWLEDGMENTS

We thank O. G. Mouritsen for useful comments on the manuscript. One of us (T.C.) wishes to thank Risø National Laboratory for the hospitality and Comissió Interdepartamental de Recerca i Innovació Tecnològica (CIRIT) of the Catalan Government for financial support.

APPENDIX: THE PINNING CENTER

The behavior and the reason for the pinning center in model II is discussed further in this Appendix. The energy gain for models I and II lies, first, in the reduction of the length L_S of the S boundary. The pinning centers do not move at low temperatures, but L_S is reduced until the two connecting C boundaries form an optimum angle close to 120°, both between the S and C boundaries and between the meeting C boundaries (see Fig. 6). After this configuration is reached, the time evolution effectively stops. To illustrate this we have simulated the evolution of test cases as shown in the insets of Fig. 9, where we have plotted the motion of the C boundary for the model I with no pinning and for model II with the pinning center. Contrary to the temporary pinning exhibited by the S boundary, which can be removed when $L_S\rightarrow 0$, we are here in the combination dealing with a drastic pinning, which cannot be removed by other wall motions. The pinning center consists of two abruptly broken chains. This has a low energy $E(a)$ than the energy of two soliton walls meeting directly $E_{\downarrow\uparrow}$ [see Fig. 10(a)]. Let us now analyze two possible movements of the pinning centers.

They may either (i) expand along the C boundaries or (ii) hop in favorable direction for the C-boundary movement in order to reduce L_S. The movement (i) does not reduce any boundary length, i.e., there is no major driving force. Nevertheless, it interacts with the dynamics of the walls. In Fig. 10(a) we show the distribution of solitons around the pinning center in the pinned configuration as in Fig. 6. The energy of the configuration $E(a)$ is given in Fig. 10(e). The energy de-

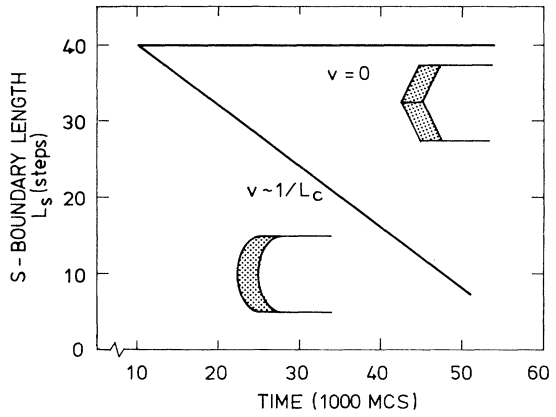

FIG. 9. The time evolution from a MC simulation of (lower inset) an unpinned broad C boundary moving with velocity $v \sim 1/L_C$ and (upper inset) a pinned wall, for which no move was observed, i.e., $v = 0$.

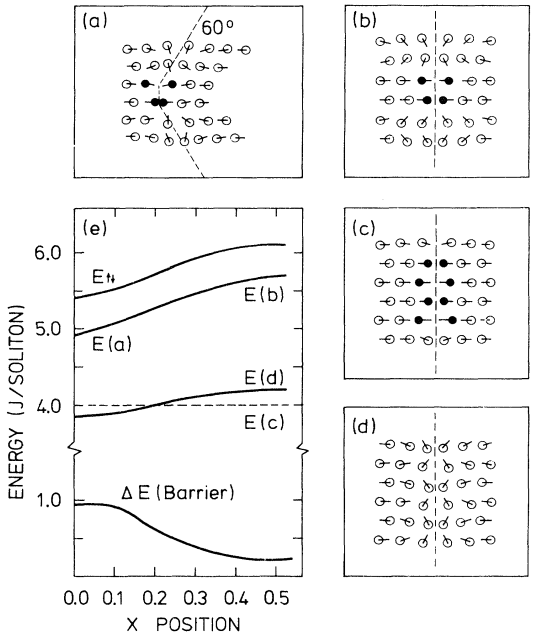

FIG. 10. (a) The optimum-angle configuration of a pinning center with energy $E(a)$. (b) The pinning in a weakly curved or straight situation with energy $E(b)$. (c) An expanding pinning point which is converting the soliton walls into sharp C walls with energy $E(c)$. (d) The straight soliton wall configuration with no pinning point with energy $E(d)$. (e) These energies are compared. In addition, the energy $E_{\uparrow\downarrow}$ is given for a direct meeting of two oppositely pointing soliton walls, and the barrier $\Delta E_{\text{barrier}}$ between the broad and sharp C boundaries.

pends on the position x between two lattice sites of the maximum for the neighboring solitons in Fig. 10(a). An expansion of the pinning center is possible when the C walls are fairly straight [Fig. 10(b)], i.e., have not reached the optimum-angle configuration [Fig. 10(a)]. An expansion can take place provided that the lengths of the connection C boundaries are long enough. If they are too short, the system will evolve too rapidly and be trapped in the pinned case [Fig. 10(a)]. For configuration (b) [Fig. 10(b)], the energy is $E(b)$ [Fig. 10(e)]. This is slightly higher than $E(a)$. The energy can be decreased by converting the neighboring soliton walls to sharp walls as shown in Fig. 10(c). The energy $E(d)$ for a soliton wall was previously[13] found to depend on x with a value between $3.9J$ and $4.1J$. The sharp C wall has an energy $E(c)=4J$ independent of x. A sharp C wall is therefore generally favorable for C boundaries with small curvature, as shown in Fig. 10(e). However, the sharp-wall energy minimum is separated[13] from the broad-wall minimum by the energy barrier $\Delta E_{\text{barrier}}$ indicated at the bottom of Fig. 10(e). It has a minimum of $0.2J=0.08T_C$. Therefore only at temperatures above $T>0.08T_C$ can the fairly straight C boundaries have a reasonable probability of being converted into sharp walls, thereby gaining energy. If during such an expansion of the sharp C walls, one pinning center collides with another, both mutually annihilate. The whole C wall then optimizes the energy by jumping back to the broad, curved configuration, which is unpinned with an energy $E(d)$. This wall is unpinned and can move. The same happens if the expanding sharp C wall meets an S boundary. When the pinning centers cannot be eliminated by one of these processes, the C boundary will be trapped in the optimum angle configuration [Fig. 10(a)]. The described behavior is observed in the simulations. For the case (ii), the energy barrier for the pinning center to hop in the favorable direction perpendicular to the C boundary is $2J$. It corresponds to inverting one of the oppositely aligned spins. This is a very high barrier compared to the others discussed, and a jump is therefore very unlikely at low temperatures. However, by also flipping the neighbor spin, the energy cost of the two-flip event is close to zero. At higher temperatures, the two-flip process is possible; therefore, both this mechanism and the elimination process become operative, and the pinning of the C boundaries ceases. The temperature dependence of the effective exponents clearly shows this (Fig. 5).

[1]O. G. Mouritsen and E. Præstgaard, Phys. Rev. B **38**, 2703 (1988).
[2]O. G. Mouritsen and P. J. Shah, Phys. Rev. B **40**, 11 445 (1989).
[3]D. J. Srolovitz and G. N. Hassold, Phys. Rev. B **35**, 6902 (1987).
[4]D. A. Huse and C. L. Henley, Phys. Rev. Lett. **54**, 2708 (1985).
[5]K. Kaski, T. Ala-Nissilä, and J. D. Gunton, Phys. Rev. B **31**, 310 (1985).
[6]T. Ala-Nissilä, J. D. Gunton, and K. Kaski, Phys. Rev. B **33**, 7583 (1986).

[7]M. P. Anderson, D. J. Srolovitz, G. S. Grest, and P. S. Sahni, Acta Metall. **32**, 783 (1984).
[8]D. J. Srolovitz, M. P. Anderson, P. S. Sahni, and G. S. Grest, Acta Metall. **32**, 7, 93 (1984).
[9]A. Sadiq and K. Binder, J. Stat. Phys. **35**, 517 (1984).
[10]G. C. Wang and T. M. Lu, Phys. Rev. Lett. **50**, 2014 (1983).
[11]S. M. Allen and J. W. Cahn, Acta Metall. **27**, 1085 (1979).
[12]O. G. Mouritsen, Phys. Rev. B **28**, 3150 (1983); Phys. Rev. Lett. **56**, 850 (1986); Phys. Rev. B **31**, 2613 (1985).
[13]T. Castán and P.-A. Lindgård, Phys. Rev. B **40**, 5069 (1989); P.-A. Lindgård and T. Castán, *ibid.* **41**, 4659 (1990).
[14]T. Castán and P.-A. Lindgård, Phys. Rev. B **41**, 2534 (1990).
[15]P.-A. Lindgård and O. G. Mouritsen, Phys. Rev. B **41**, 688 (1990).
[16]S. A. Safran, Phys. Rev. Lett. **46**, 1581 (1981).
[17]G. S. Grest, M. P. Anderson, and D. J. Srolovitz, Phys. Rev. B **38**, 4752 (1988); P. S. Sahni, G. S. Grest, M. P. Anderson, and D. J. Srolovitz, Phys. Rev. Lett. **50**, 263 (1983).
[18]For a review, see J. D. Gunton, M. San Miguel, and P. S. Sahni, in *Phase Transitions and Critical Phenomena,* edited by C. Domb and J. L. Lebowitz (Academic, New York, 1983), Vol. 8, p. 269.
[19]K. Kaski, S. Kumar, J. D. Gunton, and P. A. Rikvold, Phys. Rev. B **29**, 4420 (1984).
[20]E. T. Gawlinski, M. Grant, J. D. Gunton, and K. Kaski, Phys. Rev. B **31**, 281 (1985).
[21]G. S. Grest and D. J. Srolovitz, Phys. Rev. B **32**, 3014 (1985); D. J. Srolovitz and G. S. Grest, *ibid.* **32**, 3021 (1985).
[22]M. Grant and J. D. Gunton, Phys. Rev. B **35**, 4922 (1987); S. R. Anderson, *ibid.* **36**, 8435 (1987).
[23]O. G. Mouritsen, Phys. Rev. B **32**, 1632 (1985); G. F. Mazenko and O. T. Valls, *ibid.* **33**, 1823 (1986); and T. Otha, K. Kawasaki, A. Sato, and Y. Enomoto, Phys. Lett. A **126**, 93 (1987).
[24]A. Milchev, K. Binder, and D. W. Heermann, Z. Phys. B **63**, 521 (1986).
[25]J.-K. Zuo, G.-C. Wang, and T.-M. Lu, Phys. Rev. Lett. **60**, 1053 (1988).
[26]R. F. Shannon, C. R. Horkless, and S. E. Nagler, Phys. Rev. B **38**, 9327 (1988).
[27]G. F. Bolling and W. C. Wineyard, Acta Metall. **6**, 283 (1958).
[28]J. P. Drolet and A. Galibois, Acta Metall. **16**, 1387 (1968).
[29]P. Gordon and T. A. El-Basyoumi, Trans. Metall. Soc. AIME **233**, 391 (1965).
[30]P.-A. Lindgård, H. E. Viertiö, and O. G. Mouritsen, Phys. Rev. B **38**, 6798 (1988).
[31]P.-A. Lindgård and O. G. Mouritsen, Phys. Rev. Lett. **57**, 2458 (1986).
[32]O. G. Mouritsen, in *Computer Studies of Phase Transitions and Critical Phenomena,* edited by H. Cabanes, M. Holt, H. B. Keller, J. Killeen, J. A. Orszag, and V. V. Rusanov (Springer-Verlag, Heidelberg, 1984).
[33]K. Binder, in *Applications of Monte Carlo Methods in Statistical Physics,* edited by K. Binder (Springer-Verlag, Heidelberg, 1984).
[34]G. S. Grest and D. J. Srolovitz, Phys. Rev. B **30**, 6535 (1984).
[35]K. Kaski, M. Grant, and J. D. Gunton, Phys. Rev. B **31**, 3040 (1985).
[36]W. van Saarloos and M. Grant, Phys. Rev. B **37**, 2274 (1988).